

Distinguishing the 3 primitive 3D-topological configurations: simplex, hole, tunnel *

Abstract With most of the work focussing on 2D representations, topology preserving hierarchies have received a lot of attention. Concepts for extending such representations to handle any dimension have also been the subject of active research in the recent years, but very little work has been done to collapse a huge amount of volumetric data into its minimal topologically equivalent data structure. This paper presents 3D combinatorial maps and the primitive operations needed to simplify such a representation. Minimal configurations of the three primitive topological configurations, simplex, hole, and tunnel, are studied. First experimental results and possible applications show the potential of the approach.

1 Introduction

Handling “structured geometric objects” is important for many applications related to geometric modeling, computational geometry, image analysis, etc.; one has often to distinguish between different parts of an object, according to properties which are relevant for the application (e.g. mechanical, photometric, geometric properties).

For instance for geological modeling, the sub-ground is made of different layers, maybe split by faults, so layers are sets of (maybe not connected) geological blocks.

For e.g. in image analysis, a region is a (structured) set of pixels or voxels, or more generally an abstract cellular complex consisting of dimensions 0, 1, 2, 3 ... (i.e. 0-cells are vertices, 1-cells are edges, 2-cells are faces, 3-cells are volumes, ...) and a bounding relation [17].

The structure, or the topology, of the object is related to the decomposition of the object into sub-objects, and to the relations between these sub-objects.

Basically, topological information is related to the cells and their adjacency and bounding relations. Other information (embedding information) are associated to these sub-objects, and describe for instance their shapes (e.g. a point, resp. a curve, a part of a surface, is associated with each vertex, resp. each edge, each face), their textures or colors, or other information depending on the application.

Many topological models have been conceived for representing the topology of subdivided objects, since differ-

* This paper was supported by the Austrian Science Fund under grant FSP-S9103-N04.

ent types of subdivisions have to be handled: general complexes [8, 9] or particular manifolds [1, 2], subdivided into any cells [14, 12] or into regular ones (e.g. simplices, cubes, etc.) [13, 20]. Few models are defined for any dimensions [3, 21, 5, 19]. Some of them are (extensions of) incidence graphs or adjacency graphs. Their principle is often simple, but

- they cannot deal with any subdivision without loss of information, since it is not possible to describe the relations between two cells precisely if they are incident in several locations;
- operations for handling such graphs are often complex, since they have to handle simultaneously different cells of different dimensions.

Other structures are “ordered” [5, 19], and they do not have the drawbacks of incidence or adjacency graphs. A subdivided object can be described at different levels, so several works deal with hierarchical topological models and topological pyramids [11, 3, 18]. For geometric modeling, levels are often not numerous. For image analysis, more levels are needed since the goal is to rise up information which is not known a priori.

[7, 15] show that 2D combinatorial maps are suitable topological structures to be used in 2D segmentation. Many domains need to work in 3D imagery (e.g. medicine, geology), so the theoretical framework of 2D combinatorial maps has been extended to 3D [10, 4]. In order to use 3D topological structures for 3D image segmentation one has to define basic operations. In this paper only two basic operations are introduced: the contraction and the removal operation.

Attempts have been made to reduce such representations [10] to a certain extent, without guaranteeing the minimal representation. We extend this work in order to find minimal representations of the topological configurations of the initial data. And distinguish between them using the remaining pseudo-elements.

A short introduction of the 2D and 3D combinatorial map is given in Section 2. In Section 3 the two operations, namely contraction and removal, are properly applied to three objects. We show examples of the three basic structures in 3D: a simply connected volume, a volume with a hole (volume enclosing other volume), and a volume with

121 a tunnel (donut) and their minimal configurations that pre-
 122 serve the topology.

123
 124 **2 Combinatorial Maps**

125 *Combinatorial maps* and *generalized maps* define a general
 126 framework which allows us to encode any subdivision of
 127 nD topological spaces orientable or non-orientable with or
 128 without boundaries. They encode all the incidence relations
 129 and consist of abstract elements, called darts \mathcal{D} and a set of
 130 permutations β_i . i -cells are implicitly encoded by subsets of
 131 \mathcal{D} which can be obtained using the β_i permutations. (When
 132 encoding the same configuration, differences between the
 133 two mentioned map types are limited to the number of darts,
 134 number of permutations, and their meaning).

135
 136 In the case of combinatorial maps, for each dimension,
 137 there is more than one way of attributing the permutations,
 138 but the number of permutations used for a certain dimension
 139 and how many of them are involutions is fixed i.e. for an
 140 nD combinatorial map there is 1 permutation and $n - 1$
 141 involutions (an involution is a permutation whose orbits are
 142 of size 1 or 2).

143 2D and 3D combinatorial maps are given in more detail
 144 in the following sections.

145 **2.1 2D Combinatorial Maps**

146 2D Combinatorial maps may be understood as a particular
 147 encoding of a planar graph, where each edge is split into two
 148 half-edges, the so called darts. A 2D combinatorial map is
 149 formally defined by the triplet $G = (\mathcal{D}, \sigma, \alpha)$ [6] where \mathcal{D}
 150 represents the set of darts, σ is a permutation on \mathcal{D} encoun-
 151 tered when turning clockwise around each vertex (the cycles
 152 of σ encode the vertices), and α is an involution on \mathcal{D} which
 153 maps each of the two darts of one edge to the other one (the
 154 cycles of α encode the edges). The cycles of the permutation
 155 φ , defined as $\varphi = \sigma \circ \alpha$, encode the faces of the combina-
 156 torial map. (see Fig. 1d) [10] uses β_1 to refer to φ and β_2
 157 to refer to α and represents the 2D combinatorial map as
 158 $G = (\mathcal{D}, \beta_1, \beta_2)$ (see Fig. 1b).

160 **2.2 3D Combinatorial Maps**

161 A 3D combinatorial map is formally defined by
 162 $G = (\mathcal{D}, \text{permutation}, \text{involution}_1, \text{involution}_2)$,
 163 with the following two notations (and meanings) for the
 164 permutations studied until now: $G = (\mathcal{D}, \beta_1, \beta_2, \beta_3)$ [4]
 165 and $G = (\mathcal{D}, \gamma, \sigma, \alpha)$ [4]. Further on, we will present the
 166 first one.

167 Like in the similar 2D combinatorial map notation, the
 168 permutation β_1 connects darts belonging to the same face
 169 and the same volume, preserving their ordering on the
 170 boundary of the face, and the involution β_2 connects 2 darts,
 171 part of the same edge and the same volume. The additional
 172 involution, β_3 , links 2 darts that belong to the same face and
 173 same edge (and the 2 volumes separated by the respective
 174 face). β_3 can be regarded like a glue, which brings together
 175 neighboring volumes defined by the 2D manifolds encoded
 176 by β_1 and β_2 (see Fig. 2).

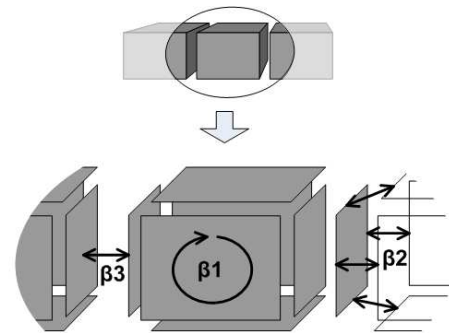
177 For a certain dart d , the set of darts implicitly represent-
 178 ing the i -cell containing the dart d is obtained by applying
 179 2 of the 3 permutations β_i any number of times and in any
 180

combination to the dart d . (i is defined by the 2 permutations
 applied) [4].

181
 182
 183 **2.2.1 Operations on the 3D Combinatorial Maps**

184 We apply two operations to an i -cell: removal (removes the i -
 185 cell and merges the 2 $(i+1)$ -cells that it was separating) and
 186 contraction (contracts the i -cell to a $(i-1)$ -cell by merging it's
 187 2 neighboring $(i-1)$ -cells). For our experiments we used the
 188 following 4 operations: *edge contraction*, *face contraction*,
 189 *volume contraction* and *face removal*. (See Table 1)

190 Our maps encode volumes from the input data as vertices
 191 and thus *edge contraction* is the equivalent to merging two
 192 such neighboring volumes. The other 3 operations are applied
 193 to simplify/collapse the resulting representation, while
 194 preserving the correct topological configuration. The last
 195 one (*face removal*) is needed to deal with the special case
 196 of "face self loop", which is a face that encloses a volume
 197 alone, and which is bounded by one edge. (Such a self loop
 198 can be the result of the contraction operations described).
 199



200
 201
 202
 203
 204
 205
 206
 207
 208
 209
 210
 211
 212 **Figure 2: 3D Combinatorial map permutations**

213
 214
 215 **2.2.2 Pseudo elements** To keep the topological encod-
 216 ing consistent, the simplification process keeps i -cells which
 217 help encoding inside-like relations. In 2D this means keep-
 218 ing self-loops and parallel edges which surround at least one
 219 vertex, in 3D this concept is translated as parallel faces and
 220 "face self loops" (faces bounded by a single edge) which
 221 enclose a vertex. As shown in the following sections, these
 222 pseudo elements let us discriminate between different topo-
 223 logical configurations.
 224

225 **2.2.3 Multiple minimal encodings** Every i -cell needs
 226 to be bounded by at least one $(i-1)$ -cell i.e. a volume is
 227 bounded by at least one face, a face by at least one edge, and
 228 an edge by at least 1 vertex. This leads to multiple encod-
 229 ings for the same topological configuration which cannot be
 230 reduced/collapsed anymore. For example a single volume,
 231 can be represented as a volume bounded by 2 faces bounded
 232 by the same edge (self loop) and 1 vertex (a globe obtained
 233 from gluing together 2 halves around the self loop which is
 234 the equator) (Fig. 3a), or as a volume bounded by 1 face,
 235 bounded by 1 edge connecting 2 vertices (a soap bubble
 236 hanging in the middle of the straw)(Fig. 3b). So, depend-
 237 ing on the operations applied and their order, starting from
 238 the same initial configuration, we can obtain different output
 239 configurations that are topologically equivalent.
 240

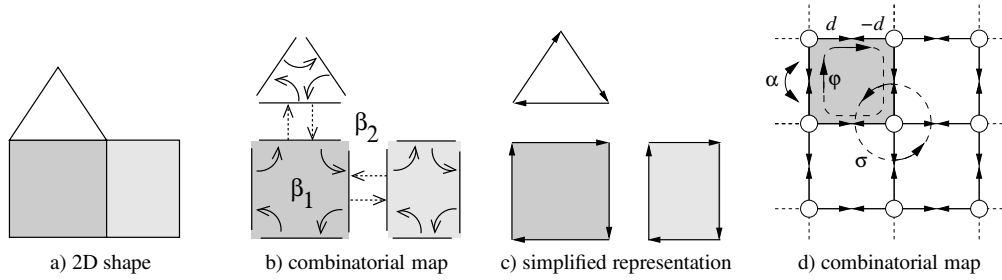


Figure 1: 2D Combinatorial maps using different notations.

Operation	Preconditions	Result
edge contraction	edge connects 2 different vertices, no volumes or faces will be removed	the 2 vertices are merged, contracted edge is removed
face contraction	face is bounded by 2 different edges no volumes or vertices will be removed	the 2 bounding edges are merged contracted face is removed
volume contraction	volume is bounded by 2 different faces no vertices or edges will be removed	the 2 bounding faces are merged the volume is removed
face removal	face is incident to 2 different volumes no vertices or edges are removed	the 2 incident volumes are merged the face is removed

Table 1: Operations applied to the 3D Combinatorial map

3 Connected component analysis

As mentioned in Section 2.2.1, in our setup voxels from the input data are represented as vertices and adjacency relations between 2 voxels are represented by connecting their 2 associated vertices by an edge. An additional vertex is used to represent the background volume. For the sake of clarity, this vertex is not drawn in the initial configuration images of our experiments.

The algorithm for identifying the connected components is as follows (each operations is applied only if the preconditions mentioned in Table 1 are satisfied):

1. contract all edges connecting two vertices that belong to the same connected component
2. contract all faces bounded by exactly two edges
3. contract all volumes bounded by exactly two faces
4. remove all "face self loops"

The four steps are repeated until Step 1 does not find any more contractable edges. In each such iteration, Steps 2-4 are repeated until neither of them finds any more candidates for contraction/removal.

3.1 2 x 2 x 2 Cube - 1 connected component

The first experiment is the reduction of a $2 \times 2 \times 2$ cube where each voxel has the same label. Fig. 4a shows the initial combinatorial map for this object. (The labels of vertices and edges correspond to the labels used by our library.) The final configuration is shown in Fig. 4b. The map is reduced to 4 darts defining 2 vertices, 2 edges, 1 face and 1 volume.

One vertex represents the background and the other one represents the voxels of the initial cube that has been merged into 1 element. These 2 vertices are connected by 1 face that is bounded by 2 edges.

3.2 3 x 3 x 3 Cube with enclosed object inside - 2 connected components

To demonstrate that the topology is preserved during the simplification of the combinatorial map, the second experiment reduces a **cube that completely encloses another object**. Fig. 4c shows the initial combinatorial map for this configuration. The two objects are reduced to a combinatorial map consisting of 16 darts defining 4 vertices, 5 edges, 3 faces and two volumes (see Fig. 4d).

The outer cube enclosing the inner object is merged into 2 vertices connected by a single edge. These 2 vertices (vertex 17 and 26) connect to the background (vertex 28) and the inner object (vertex 14). In addition the edge between these 2 vertices defines a face that completely encloses the inner object (vertex 14) representing the inclusion relation of this object being inside the outer cube.

3.3 3 x 3 x 2 Cuboid with object tunnel inside - 1 connected component

In 3D there are basically 2 types of *inside* configurations. The 3rd experiment shows the **reduction of a torus** which is surrounding (but not completely enclosing) another object. Fig. 4e shows the initial combinatorial map for this experiment. The 2 objects are reduced to a combinatorial map consisting of 24 darts defining 3 vertices, 5 edges, 4 faces and 2 volumes (see Fig. 4f).

The torus is merged into 1 vertex (vertex 17) connected to the background (vertex 19) and the inner tunnel (vertex 14). The tunnel (vertex 14) is connected on both sides with the background (edges -755 and -155). The fact that the torus surrounds the tunnel is represented by the self loop (edge -679) and the cone like face/surface (bounded by the self-loop edge -679 and the edge -826; visualized by the dotted lines).

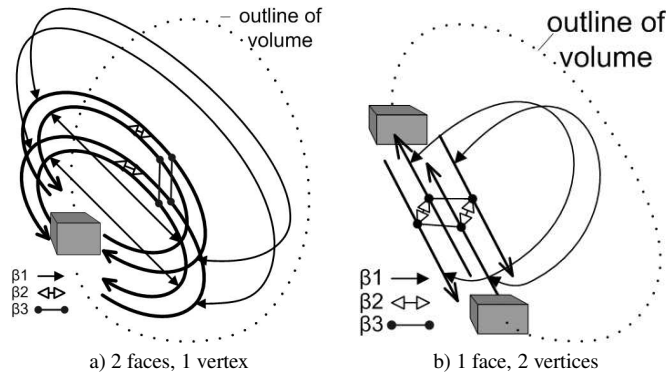


Figure 3: Multiple minimal encodings for one volume

Configuration	Darts	Vertices	Edges	Faces	Volumes
2x2x2 cube (initial)	120	9	20	18	7
2x2x2 cube (final)	4	2	2	1	1
2x2x2 cube (final - pseudo elements)			0	0	0
3x3x3 with object inside (initial)	576	28	80	84	32
3x3x3 with object inside (final)	16	4	5	3	2
3x3x3 with object inside (final - pseudo elements)			0	1	1
3x3x2 with tunnel inside (initial)	352	19	51	52	20
3x3x2 with tunnel inside (final)	24	3	5	4	2
3x3x2 with tunnel inside (final - pseudo elements)			1	1	0

Table 2: Number of cells in each experimented configuration

3.4 Discriminating between the 3 configurations

As can be seen from the experiment results, discriminating between the first configuration and the other two is very easy, and can be done just by looking at the labels of the obtained vertices. The second and third configurations are more complex, because of the containment relation and cannot be discriminated based only on the vertices. Here, edges and faces have to be taken into considerations. An object having an edge self loop (or edge cycle) surrounds another object (Fig. 4f), and an object having a face self-loop (or face cycle) encloses another one (Fig. 4d). Note that in experiment 3, the adjacency of the tunnel and the background is also shown by the 2 edges connecting it to the background.

4 Outlook

Connected component analysis is certainly one of the first experiments to do when testing out a new representation that should preserve topology, but the possibilities do not stop here. Next steps will include the extension to 3D of the Minimum Spanning Tree pyramid concept [15] used for segmentation of 2D images, and using it to segment volumetric data and videos (2D+time). Further on, having this implementation, we can pursue research in describing videos using actions, events, and relations, following the concept presented in [16].

5 Conclusions

The paper presents the basic operations that can collapse a high resolution voxel complex into its topologically equivalent smallest counterpart. We demonstrated the correctness

of the underlying software library by the three basic configurations in 3D: a simply connected volume, a volume with a hole and a volume with a tunnel. The resulting structures contain pseudo elements characterizing the respective topology.

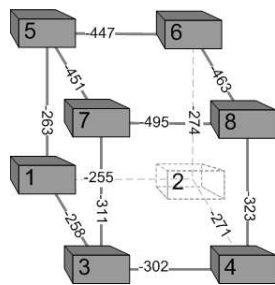
References

- [1] S. Ansal di, L. de Floriani, and B. Falcidieno. Geometric Modeling of Solid Objects by Using a Face Adjacency Graph Representation. *Computer Graphics*, 19(3):131–139, 1985.
- [2] B. Baumgart. A Polyhedron Representation for Computer Vision. In *AFIPS National Computer Conference Proc.*, volume 44, pages 589–596, Anaheim, May 1975.
- [3] Y. Bertrand, G. Damiand, and C. Fiorio. Topological Encoding of 3D Segmented Images. In G. Borgefors, I. Nyström, and G. S. di Baja, editors, *International Conference on Discrete Geometry for Computer Imagery*, volume 1953 of *Lecture Notes in Computer Science*, pages 311–324. Springer-Verlag, Germany, 2000.
- [4] A. Braquelaire, G. Damiand, J-P. Domenger, and F. Vidil. Comparison and convergence of two topological models for 3d image segmentation. In *Workshop on Graph-Based Representations in Pattern Recognition*, number 2726 in *Lecture Notes in Computer Science*, pages 59–70, York, England, June 2003.
- [5] E. Brisson. Representing Geometric Structures in D Dimensions: Topology and Order. *Discrete and Computational Geometry*, 9:387–426, 1993.
- [6] Luc Brun and Walter G. Kropatsch. Dual Contraction

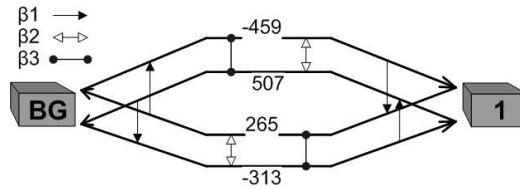
481	of Combinatorial Maps. Technical Report		
482	PRIP-TR-54, Institute f. Computer Aided Automation	[19]	P. Lienhardt. N-dimensional Generalized
483	183/2, Pattern Recognition and Image Processing		Combinatorial Maps and Cellular Quasi-manifolds.
484	Group, TU Wien, Austria, 1999. Also available		<i>Int. J. of Comp. Geom. and Appl.</i> , 4(3):275–324, 1994.
485	through	[20]	A. Paoluzzi, F. Bernardini, C. Cattani, and V. Ferrucci.
486	http://www.prip.tuwien.ac.at/ftp/pub/publications/trs/tr54.ps.gz .		Dimension Independent Modeling with Simplicial
487	[7] Luc Brun and Walter G. Kropatsch. Irregular		Complexes. <i>ACM Trans. on Graphics</i> , 12(1):56–102, 1993.
488	Pyramids with Combinatorial Maps. In Francesc J.	[21]	J. Rossignac and M. O’Connor. SGC: a
489	Ferri, José M. Iñesta, Adnan Amin, and Pavel Pudil,		Dimension-independent Model for Pointsets with
490	editors, <i>Advances in Pattern Recognition, Joint IAPR</i>		Internal Structures and Incomplete Boundaries. In
491	<i>International Workshops on SSPR’2000 and SPR’2000</i> , volume		M. J. Wozny, J. Turner, and K. Preiss, editors, <i>In</i>
492	1876 of <i>Lecture Notes in Computer Science</i> , pages 256–265,		<i>Geometric Modeling for Product Engineering</i> , pages 145–180.
493	Alicante, Spain, August 2000. Springer, Berlin		Elsevier Science, 1989.
494	Heidelberg, New York.		
495	[8] P. Cavalcanti, P. Carvalho, and L. Martha.		
496	Non-manifold Modeling: An Approach Based on		
497	Spatial Subdivision. <i>Computer-Aided Design</i> ,		
498	29(3):209–220, 1997.		
499	[9] G.A. Crocker and W.F. Reinke. An Editable		
500	Nonmanifold Boundary Representation. <i>Computer</i>		
501	<i>Graphics and Applications</i> , 11(2):39–51, 1991.		
502	[10] G. Damiand. <i>Définition et étude d’un modèle topologique</i>		
503	<i>minimal de représentation d’images 2d et 3d</i> . Thèse de		
504	doctorat, Université Montpellier II, Décembre 2001.		
505	[11] L. De Floriani, E. Puppo, and P. Magillo. A Formal		
506	Approach to Multiresolution Hypersurface Modeling.		
507	In R. Straber, W. and Kein and R. Rau, editors,		
508	<i>Geometric Modeling: Theory and Practice</i> , pages 302–323.		
509	Springer-Verlag, 1997.		
510	[12] D. Dobkin and M. Laszlo. Primitives for the		
511	manipulation of three-dimensional subdivisions.		
512	<i>Algorithmica</i> , 4(1):3–32, 1989.		
513	[13] V. Ferruci and A. Paoluzzi. Extrusion and Boundary		
514	Evaluation for Multidimensional Polyhedra.		
515	<i>Computer-Aided Design</i> , 23(1):40–50, 1991.		
516	[14] L. Guibas and J. Stolfi. Primitives for the		
517	Manipulation of General Subdivisions and the		
518	Computation of Voronoi Diagrams. <i>ACM Trans. on</i>		
519	<i>Graphics</i> , 4(2):74–123, 1985.		
520	[15] Yll Haxhimusa, Adrian Ion, Walter G. Kropatsch, and		
521	Luc Brun. Hierarchical Image Partitioning using		
522	Combinatorial Maps. In D. Chetverikov, L. Czuni,		
523	and M. Vincze, editors, <i>Joint Hungarian-Austian Conference</i>		
524	<i>on Proceedings on Image Processing and Pattern Recognition,</i>		
525	<i>HACIPPR 2005 - OAGM 2005/KPAF 2005</i> , pages 179–186,		
526	Veszprm, Hungary, 11-13, May 2005. OCG.		
527	[16] Adrian Ion, Yll Haxhimusa, and Walter G. Kropatsch.		
528	A Graph-Based Concept for		
529	Spatiotemporal Information in Cognitive Vision. In		
530	L. Brun and M. Vento, editors, <i>5th IAPR-TC15 Workshop</i>		
531	<i>on Graph-based Representation in Pattern Recognition</i> , volume		
532	3434 of <i>Lecture Notes in Computer Science</i> , pages 223–232,		
533	Poitiers, France, April 2005. Springer, Berlin		
534	Heidelberg, New York.		
535	[17] Vladimir A. Kovalevsky. Finite topology as applied to		
536	image analysis. <i>Computer Vision, Graphics, and Image</i>		
537	<i>Processing</i> , 46:141–161, 1989.		
538	[18] W.G. Kropatsch. Building Irregular Pyramids by Dual		
539	Graph Contraction. <i>IEE-Proc. Vision, Image and Signal</i>		
540			

601
602
603
604
605
606
607
608
609
610
611
612
613
614
615
616
617
618
619
620
621
622
623
624
625
626
627
628
629
630
631
632
633
634
635
636
637
638
639
640
641
642
643
644
645
646
647
648
649
650
651
652
653
654
655
656
657
658
659
660

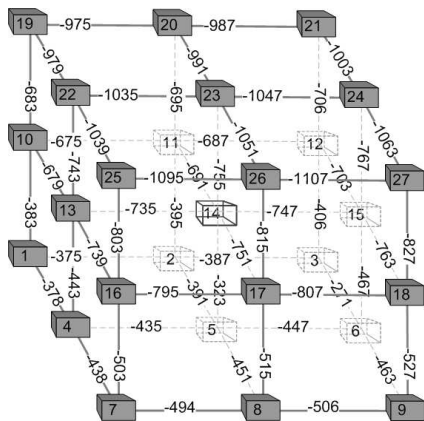
—661
—662
—663
—664
—665
—666
—667
—668
—669
—670
—671
—672
—673
—674
—675
—676
—677
—678
—679
—680
—681
—682
—683
—684
—685
—686
—687
—688
—689
—690
—691
—692
—693
—694
—695
—696
—697
—698
—699
—700
—701
—702
—703
—704
—705
—706
—707
—708
—709
—710
—711
—712
—713
—714
—715
—716
—717
—718
—719
—720



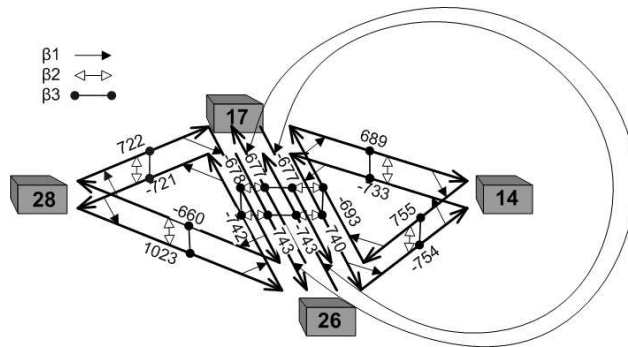
a) $2 \times 2 \times 2$ initial map



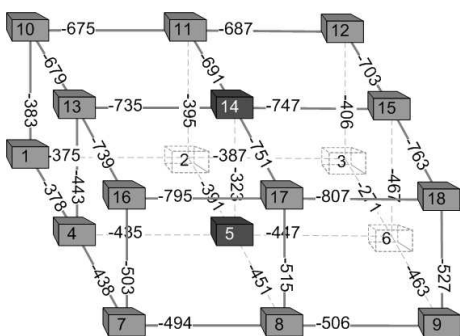
b) $2 \times 2 \times 2$ final map



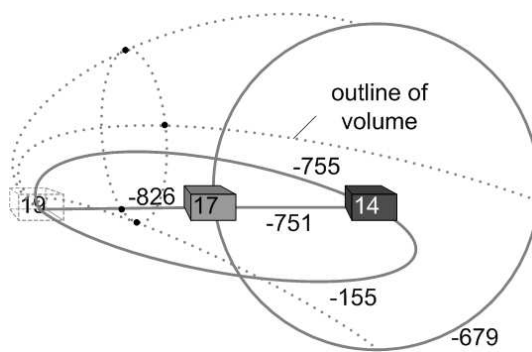
c) $3 \times 3 \times 3$ initial map



d) $3 \times 3 \times 3$ final map



e) $3 \times 3 \times 2$ initial map



f) $3 \times 3 \times 2$ final map

Figure 4: The 3 primitive 3D topological configurations: simplex(a,b), hole(c,d), tunnel(e,f)